Contributed paper

OPTO-ELECTRONICS REVIEW **12**(2), 213–219 (2004)

Two-layer responsivity modelling of HgCdTe photoconductive detectors

R.K. BHAN* and V. DHAR

Solid State Physics Laboratory, Lucknow Road, 110054 Delhi, India

This paper presents a simple two-layer responsivity model of n-HgCdTe photoconductive detectors by including the contribution of shunt resistance arising due to the accumulation layer at the surface. It is shown that in general responsivity of a proper two-layer model is higher than quasi two-layer model that is reported in literature and used by many workers.

Keywords: Hg CdTe photoconductive detectors, two-layer responsity model, shunt resistance.

1. Introduction

The basic simplified relation of voltage responsivity valid for bulk n-HgCdTe (MCT) photoconductive (PC) detectors was initially given by Broudy and Mazurczyk [1] as follows

$$R_{V,b} = \left(\frac{v_b}{A_d t}\right)\left(\frac{\lambda}{hc}\right)\eta\tau_{eff}\,\frac{1}{n_b}, \tag{1}$$

where v_b is the bias across the detector, n_b is the free bulk electron concentration, A_d is the detector area, t is the thickness, λ is the wavelength of incident radiation, h is the Planck's constant, c is the velocity of light, η is the quantum efficiency of the detector and τ_{eff} is the effective minority carrier lifetime. The responsivity of these detectors, including the contribution of shunt resistance R_s, was originally modelled by Reine *et al*. [2] and subsequently used by many workers [3–6]. This shunt resistance arises due to the accumulation layer present at the surface of these detectors that is induced due to the presence of positive fixed charges at the interface of anodic oxide used to passivate these detectors. The equation given by Reine *et al*. is the modification of Eq. (1) in the sense that it is cast in terms of the effective detector resistance R_d being parallel combination of bulk and shunt resistance and the field E_{bias} across the detector as follows

$$R_{V,Reine} = \frac{\lambda\eta q}{hc}\,\frac{R_d\mu_{eb}E_{bias}\tau_{eff}}{l}, \tag{2}$$

where R_d is

$$R_d = \frac{l}{qWt\left(n_b\mu_{eb} + \dfrac{Q_{ss}}{t}\mu_{es}\right)} \tag{3}$$

In this model, R_s is modelled by two fitting parameters: the areal majority carrier density at the surface Q_{ss} and the surface mobility μ_{es}. It is a two-layer model in the sense that it defines a surface and a bulk layer, with different resistances. However, it is essentially a one-layer model, as regards responsivity, since the detector resistance (that is used to calculate the responsivity) is simply replaced by parallel combination of bulk and shunt resistance. However, the relative weightage of the bulk and shunt (surface) resistance should involve the thicknesses of these two layers. So, Reine's model is an 'effective' one- -layer model for responsivity, in which the two contributions are a priori given equal weightage, which does not seem reasonable. Note that in Eq. (3), the effect of the surface has indeed been included, in terms of Q_{ss} and μ_{es}, but the explicit weightage of the surface layer thickness t_s relative to the bulk thickness t has not been included.

Another, difficulty with this model, although it is mathematically correct, lies in the physical principles behind it. In this model, the surface carrier concentration is defined in terms of the areal density Q_{ss}, and the shunt resistance becomes independent of the surface layer thickness t_s. This approximation is valid provided $t_s << t$, the detector thickness, and in this approximation the surface layer thickness drops out. In a previous step model, we have explicitly identified t_s with the Debye length [7]. We feel that it is more physical to be explicit about the surface layer thickness, even though the approach of Reine is mathematically correct. However, as we will show later, the accumulation (surface) layer thickness for n-HgCdTe PC detectors is of the order of 0.5 μm. That is, neglecting this in the bulk layer resistance (thickness 10 μm) leads to an error of ~5% in thickness alone. As it will be shown here, the majority carrier concentration (electrons) n_s has a sharply increasing profile towards the interface. This is what motivates the present work in which we specifically calculate the profile of the majority carrier concentration as a function of the surface potential (or equivalently Q_{ss}).

*e-mail: bhan/sspl@ssplnet.org

The present paper presents a simple two-layer (2L) model which shows that in general responsivity is higher compared to bulk model.

2. Theoretical

2.1. Two-layer responsivity model

Figure 1 shows the schematic of the device model used here. The derivation is based on the approach followed for calculation of bulk responsivity model given in Ref. 8. Assuming different conductivities for the bulk and surface, we have

$$\sigma_b = qn_b\mu_{eb} + qp_b\mu_{hb}, \tag{4a}$$

$$\sigma_s = qn_s\mu_{es} + qp_s\mu_{hs}. \tag{4b}$$

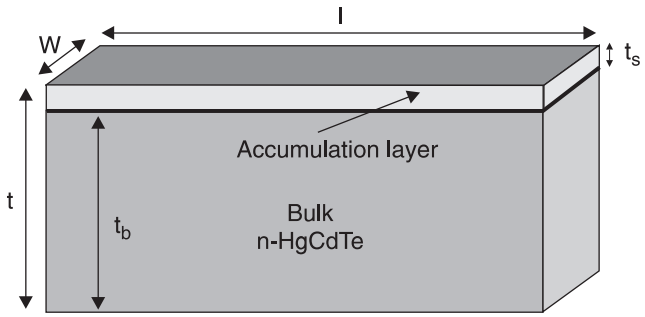

Fig. 1. Schematic of the device model showing the bulk and the surface.

The symbols have their usual meanings as given in Ref. 8. Using the parallel law of resistances in Fig. 1 we have

$$t\sigma_o = t_b\sigma_b + t_s\sigma_s, \tag{5}$$

where σ_o is the total dark conductance of the device including bulk and surface. After illumination, there will be incremental increase in conductivity such that total illuminated conductivity σ is

$$t\sigma = t\sigma_o + t\Delta\sigma, \tag{6}$$

which on substitution from Eq. (5) reduces to

$$\begin{aligned} t\sigma = {} & q[t_b(n_b\mu_{eb} + p_b\mu_{hb}) + t_s(n_s\mu_{es} + p_s\mu_{hs})] \\ & + q[t_b(\Delta n_b\mu_{eb} + \Delta p_b\mu_{hb}) + t_s(\Delta n_s\mu_{es} + \Delta p_s\mu_{hs})]. \end{aligned} \tag{7}$$

Assuming $\Delta n_b = \Delta p_b$ and $\Delta n_s = \Delta p_s$ and expressing Eq. (7) in the form of Eq. (6) we have

$$t\sigma = t\sigma_o + q[t_b(\mu_{eb} + \mu_{hb})\Delta n_b + t_s(\mu_{es} + \mu_{hs})\Delta n_s] \tag{8}$$

Further, change in the carrier concentration Δn (total thickness t), Δn_b (bulk layer t_b) and Δn_s (surface layer t_s) caused signal photons being absorbed by these layers having conductivities σ, σ_b, and σ_s, can be expressed as

$$\Delta n = \frac{\eta Q_B \tau}{A_d t}, \tag{9a}$$

$$\Delta n_b = \frac{\eta_b Q_B \tau_b}{A_d t_b}, \tag{9b}$$

$$\Delta n_s = \frac{\eta_s Q_B \tau_s}{A_d t_s}, \tag{9c}$$

where η, η_b and η_s are the quantum efficiencies, τ, τ_b, and τ_s are the carrier lifetimes of total, bulk and surface layers, respectively, and Q_B is the photon flux rate (photons s^{-1}). Using Eq. (9a), (9b) and (9c) can be expressed in terms of Δn as follows

$$\Delta n_b = f_b\Delta n, \tag{10a}$$

$$\Delta n_s = f_s\Delta n, \tag{10b}$$

where $f_b = (\eta_b\tau_b t)/(\eta\tau t_b)$ and $f_s = (\eta_s\tau_s t)/(\eta\tau t_s)$. Substituting Eqs. (10a) and (10b) in Eq. (8) we have

$$\sigma = \sigma_o + \Delta\sigma, \tag{11}$$

$$\Delta\sigma = \frac{q}{t}[t_b(\mu_{eb} + \mu_{hb})f_b + t_s(\mu_{es} + \mu_{hs})f_s]\Delta n. \tag{12}$$

Now, by substitution we can get the relative change in conductivity by

$$\frac{\Delta\sigma}{\sigma} = \frac{q}{t\sigma}[t_b(\mu_{eb} + \mu_{hb})f_b + t_s(\mu_{es} + \mu_{hs})f_s]. \tag{13}$$

This is the change in conductivity due to the presence of signal photons Q_B on detector's active area. The total effective detector resistance R_d in terms of its dimensions, using Fig. 1 is given by

$$R_d = \frac{1}{\sigma tW}. \tag{14}$$

The differential form of Eq. (14) can be written as

$$dR_d = -R_d\frac{d\sigma}{\sigma}. \tag{15}$$

Substituting Eq. (15) in Eq. (13) and using Eqs. (10a) and (10b), we have

 © 2004 COSiW SEP, Warsaw

$$dR_d = -\left(\frac{R_d}{\sigma}\right)\left(\frac{q}{t}\right) \times [t_b(\mu_{eb}+\mu_{hb})f_b + t_s(\mu_{es}+\mu_{hs})f_s]\frac{\eta Q_{B(W)}\tau}{\left(\frac{hc}{\lambda}\right)(A_d t)}, \quad (16)$$

where $Q_{B(W)}$ is the photon signal radiant power in watts and is related to Q_B as follows

$$Q_{B(W)} = \frac{Q_B}{hc/\lambda}. \quad (17)$$

In order to sense the photo-generated resistance change, the device must be biased. Using the standard bias circuit with a load resistance as R_L as discussed in Ref. 8 and following the analysis given therein, the two-layer voltage responsivity $R_{V,2L}$ is given by

$$R_{V,2L} = Iq\frac{R_L R_D}{R_L + R_D} \times \frac{[t_b(\mu_{eb}+\mu_{hb})f_b + t_s(\mu_{es}+\mu_{hs})f_s]}{\sigma t}\frac{\eta\tau\lambda}{hcA_d t}. \quad (18)$$

This equation is similar to the one given in Ref. 7 except with additional contribution from surface conductivity. Let v_b be the bias across the detector and assuming $R_L >> R_D$, the above equation can be written as

$$R_{V,2L} = \left(\frac{v_b}{A_d t}\right)\left(\frac{\lambda}{hc}\right)(\eta\tau)q \times \left\{\frac{[t_b(\mu_{eb}+\mu_{hb})f_b + t_s(\mu_{es}+\mu_{hs})f_s]}{\sigma t}\right\}. \quad (19)$$

Using Eq. (5) and assuming that illumination is weak such that $\Delta\sigma << \sigma_o$, this can be further approximated as

$$R_{V,2L} = \left(\frac{v_b}{A_d t}\right)\left(\frac{\lambda}{hc}\right)(\eta\tau) \times \left\{\frac{[t_b(\mu_{eb}+\mu_{hb})f_b + t_s(\mu_{es}+\mu_{hs})f_s]}{[t_b(n_b\mu_{eb}+p_b\mu_{hb}) + t_s(n_s\mu_{es}+p_s\mu_{hs})]}\right\}. \quad (20)$$

As discussed in Refs. 1 and 7 and assuming $\mu_{eb} >> \mu_{hb}$ and $\mu_{es} >> \mu_{hs}$, a realistic assumption for n-type HgCdTe, above equation can be further expressed as

$$R_{V,2L} = \left(\frac{v_b}{A_d t}\right)\left(\frac{\lambda}{hc}\right)(\eta\tau)\left(\frac{t_b\mu_{eb}f_b + t_s\mu_{es}f_s}{t_b\mu_{eb}n_b + t_s\mu_{es}n_s}\right). \quad (21)$$

Substituting for f_b and f_s, we have

$$R_{V,2L} = \left(\frac{v_b}{A_d t}\right)\left(\frac{\lambda}{hc}\right)\left(\frac{\mu_{eb}\eta_b\tau_b + \mu_{es}\eta_s\tau_s}{t_b\mu_{eb}n_b + t_s\mu_{es}n_s}\right). \quad (22)$$

In Eq. (21), if $t_s \to 0$, it reduces to Eq. (1), after substituting the value of f_b. Or else, from Eq. (22), if $t_s \to 0$, i.e., the thickness of absorbing layer at the surface is reducing i.e., $\eta_s \to 0$ (because $\eta = 1 - e^{-\alpha t}$), then Eq. (22) reduces to Eq. (1). Additionally, from Eq. (22), if $\mu_{es} \to 0$, then again it reduces to Eq. (1). This means physically infinite shunt resistance can be obtained with zero surface mobility too. The above approximations demonstrate that 2L model reduces to bulk model for $t_s\mu_{es}$ or $\eta_s \to 0$ as expected. Comparing Eq. (22) with Eqs. (1) and (2), as expected, the dependencies of the thickness, lifetime, quantum efficiency etc. of surface accumulation layer are built-in. Additionally, it can be expressed in terms of Q_{ss} because the product $n_s t_s$ equals Q_{ss}. Furthermore, for $t_s/t << 1$ and $t_s n_s = Q_{ss}$, then $t_b \sim t$ and Eq. (22) reduces to Eq. (2).

Next, we try to cast Eq. (21) or Eq. (22) in terms of more useful and measurable parameters, i.e., resistances and responsivities for bulk and surface regions. Using parallel law of resistances from Fig. 1 we have

$$\frac{1}{R_d} = \frac{1}{R_b} + \frac{1}{R_s}, \quad (23)$$

where $R_b = 1/(q n_b \mu_{eb}) \times (l/t_b W)$ and $R_s = 1/(q n_s \mu_{es}) \times (l/t_s W)$. Using these equations, the effective resistance R_d can be related to bulk and surface parameters as follows

$$n_b\mu_{eb}t_b + n_s\mu_{es}t_s = \frac{l}{qWR_d}. \quad (24)$$

Substituting Eq. (24) in Eq. (21) and further substituting for f_b and f_s and after some algebraic manipulation we have

$$R_{V,2L} = R_d\left(\frac{R_{vb}}{R_b} + \frac{R_{vs}}{R_s}\right), \quad (25)$$

where

$$R_{vb} = \left(\frac{v_b}{A_d t_b}\right)\left(\frac{\lambda}{hc}\right)\eta_b\tau_b\frac{1}{n_b}, \quad (26)$$

$$R_{vs} = \left(\frac{v_b}{A_d t_s}\right)\left(\frac{\lambda}{hc}\right)\eta_s\tau_s\frac{1}{n_s} \quad (27)$$

From Eq. (25), if $R_s \to \infty$, $R_d \to R_b$ and Eq. (25) reduces to bulk 1L model, i.e., Eq. (1) or else, if $R_{vs} \to 0$, then $R_d \to R_b$ because $Q_{ss} \to 0$ by $n_s \to 0$, $t_s \to 0$ ($Q_{ss} = n_s t_s$) and Eq. (25) again reduces to bulk 1L model as expected.

2.2. Accumulation layer thickness t_s and areal charge density Q_{ss}

It is assumed that mainly the fixed surface state charge density Q_{ss} due to passivant is responsible for positive surface potential which accumulates the MCT surface (Fig. 1). The potential ψ is defined to be zero in the bulk and ψ_s at the surface. To satisfy Gauss law, majority carriers are always attracted to the surface and are confined in one dimension in a thin layer at the surface. However, they are free to move in other two directions under the influence of lateral field along the length of the detector. The relation between surface potential, space charge region and electric field can be obtained by using one-dimensional Poisson's equation

$$\frac{d^2\psi}{dz^2} = -\frac{\rho}{\varepsilon}, \tag{28}$$

where ρ is the total space charge density given by

$$\rho = -q[n(z) - n_b] + q[p(z) - p_b]. \tag{29}$$

Integrating Eq. (24) from bulk to surface gives the relation between the electric field E and the potential ψ [9]

$$E^2 = \left(\frac{2kT}{q}\right)^2 \left(\frac{qn_b\beta}{2\varepsilon_s}\right) \times \left[\frac{p_b}{n_b}(e^{-\beta\psi} + \beta\psi - 1) + (e^{\beta\psi} - \beta\psi - 1)\right], \tag{30}$$

where $\beta = q/\mathrm{kT}$, n_b, and p_b are equilibrium majority and minority carrier densities in the bulk. For the known n_b, p_b is calculated from intrinsic carrier concentration n_i. To determine electric field at the surface we let $\psi = \psi_s$

$$E_s^2 = \left(\frac{2kT}{q}\right)^2 \left(\frac{qn_b\beta}{2\varepsilon_s}\right) \times \left[\frac{p_b}{n_b}(e^{-\beta\psi_s} + \beta\psi_s - 1) + (e^{\beta\psi_s} - \beta\psi_s - 1)\right]. \tag{31}$$

According to Gauss law, the space charge areal density required to produce this field is

$$Q_{ss}(\psi_s) = \varepsilon_s E_s(\psi_s). \tag{32}$$

Equations (31) and (32) allow us to calculate the surface state charge density Q_{ss} for the given Ψ_s. In addition, majority and minority carrier profiles at the surface are given by

$$n_s = n_b \exp(\beta\psi_s), \tag{33}$$

$$p_s = p_b \exp(-\beta\psi_s). \tag{34}$$

After having obtained surface state charge density, one needs to relate these carrier profiles at the surface to distance this is depth which is done by numerical integration of surface field [Eq. (30)] as follows

$$depth(\psi) = \int_{\psi_s}^{\psi} \frac{d\psi}{E_s(\psi)}; \qquad \psi_s \geq \psi \geq 0, \tag{35}$$

The above equation gives the depth profile for a given ψ_s or Q_{ss} to be later used in calculation of n_s and layer model of shunt resistance calculation.

For consistency of calculations, the value of t_s must be calculated using Eq. (35) along with Eq. (33). It is that value of depth where varying majority carrier density (as a function of depth) approximately equals bulk value. This will be further discussed later in results and discussions.

Additionally, Eqs. (1), (2), (22) and (25) shall be used for calculation of responsivity. The values of various constants are given in Table 1.

Table1. Values of various constants used in calculations.

Detector temperature (K)	77
l (μm)	50
W (μm)	50
t (μm)	10
x	0.221
n_b (cm^{-3})	5×10^{14}
μ_b (cm^2/Vs)	1×10^{5}
τ_b (s)	1×10^{-6}
λ (μm)	10.6
E (V/cm)	10

3. Results and discussions

As discussed in introduction, one of the motivating factors for the present analysis stems from the fact that accumulation layer has sharply increasing profile of majority carrier density towards the surface. Figure 2(a) shows such profiles along with the effect of surface potential (+40 mV to +80 mV) calculated using the theory developed in Sec. 2.2. One may see from this figure that near the surface carrier concentration may be as high as 4×10^{18} cm^{-3}, about 4 orders of increase in magnitude for the value of surface potential of 60 mV. Figure 2(b) shows the log-log plot of n_s vs depth in the accumulation region. It may be seen that as expected, all the profiles decay towards limiting value of bulk carrier concentration, i.e., 5×10^{14} cm^{-3} in the present case. The thickness of the accumulation layer t_s has been taken as that value of depth wherein n (depth) approaches n_b, the difference being < 2%. This is how the transition point between bulk and surface regions is defined.

 © 2004 COSiW SEP, Warsaw

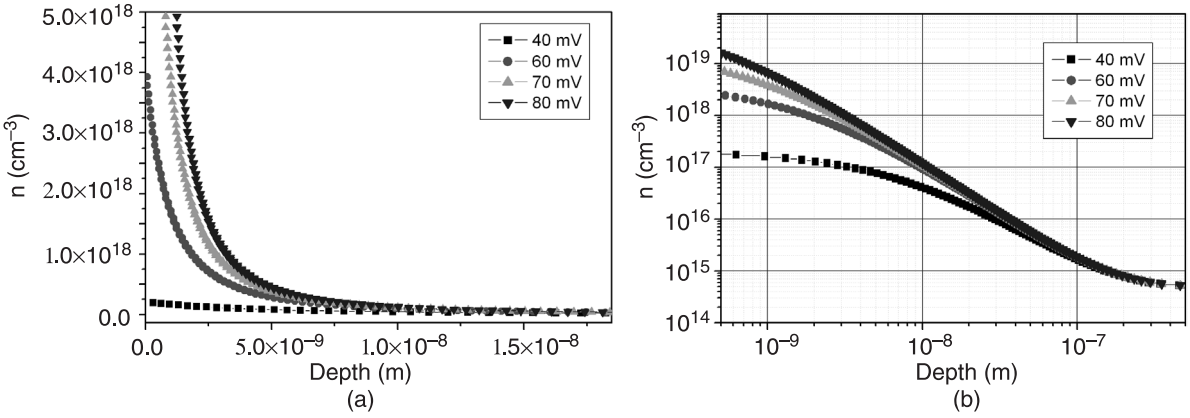

Fig. 2. (a) The depth profile of majority carrier concentration in accumulation layer near the surface. The effect of varying surface potential from 40 to 80 mV has also been depicted. (b) The view of depth profiles of carrier density in accumulation layer from surface to bulk region and showing that as expected the profiles decay to the bulk value of 5×10^{14} cm^{-3}. The depth at which n (depth) ~n_b is taken as the thickness t_s of the layer.

3.1. Effect of Q_{ss} on responsivity

In this section we try to see how the responsivity under various conditions (this is bulk, bulk corrected for surface thickness, bulk corrected for surface thickness plus shunt resistance, Reine's model and present two layer model) is affected by the varying Q_{ss}. The theory developed above for 2L case should reduce to standard bulk case (1L model) in general for the lower Q_{ss} because the surface reduces to flat band condition and R_s approaches to infinity. Figure 3(a) shows the plot of responsivity versus Q_{ss} for the above mentioned situations. As stated following four cases have been considered:

- using actual thickness $t_b = t - t_s$ for bulk resonsivity in Eqs. (25) and (26) and without considering shunt effect initially, i.e., uniform bulk material throughout, i.e., surface material properties are identical as bulk ($n_s = n_b$, $\tau_{eff} = \tau_b$ and $\eta_s = \eta_b = 1$). The idea is to depict change in responsivity due to changing t_s as a function of varying Q_{ss}. It can be seen from curve 1 of this figure that for $Q_{ss} < 1\times10^{11}$ cm^{-2} responsivity increases with increasing Q_{ss} because of increasing t_s which reduces the bulk thickness compared to its full value of 10 μm and for $Q_{ss} > 1\times10^{11}$ cm^{-2}, as expected responsivity is almost independent of Q_{ss} because for the higher t_s the various curves of Fig. 2(b) are independent of surface potential,
- curve 2 of Fig. 3(a) shows the effect of Q_{ss} on responsivity after incorporating the additional shunt resistance effect, i.e., $n_s \neq n_b$ in Eqs. (25) and (26). As it can be seen from this curve that due to increasing Q_{ss}, shunt resistance or resistance of surface layer decreases which in turn decreases responsivity drastically for typically $Q_{ss} > 1\times10^{11}$ cm^{-2}. The detector becomes totally shunt dominated for $Q_{ss} > 1\times10^{12}$ cm^{-2},
- curve 3 shows the effect of Q_{ss} on responsivity using proper 2L model using Eq. (25) assuming surface material properties are identical to bulk properties as in curve 1 or 2. The basic trend is the same as in curve 2 barring increased responsivity in for $1\times10^{9} < Q_{ss} < 1\times10^{13}$ cm^{-2}. This is due to ideal material parameters chosen for the surface, particularly unity quantum efficiency. The more realistic values shall be calculated and used in next figures later,

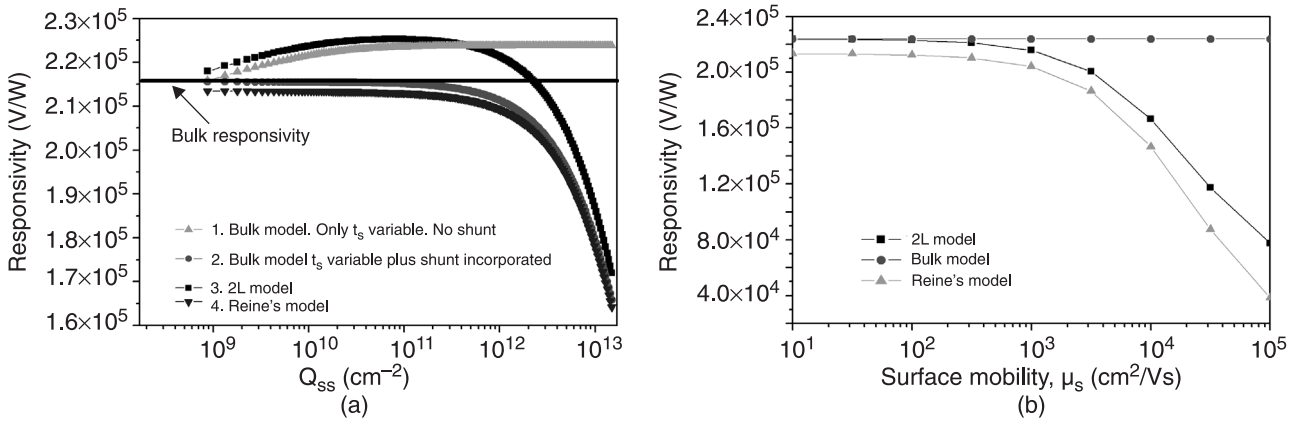

Fig. 3. (a) Plot of responsivity as a function of Q_{ss} for 2L, bulk and Reine's model. The solid line represents the bulk responsivity without shunt resistance effect and using full detector thickness of 10. (b) Plot of responsivity versus μ_{es} for 2L, bulk and Reine's model showing that 2L approaches bulk model for low Q_{ss} nearing flat band conditions.

- curve 4 shows the Reine's model for comparison purposes. In the Q_{ss} range of 1×10^{10} to 1×10^{13} cm^{-2} (practical range), Reine's model shows lower values of responsivity compared to true 2L model and for $Q_{ss} > 1\times10^{13}$ cm^{-2}, the detector is essentially strongly shunt dominated and both models tend to agree. Hence, for highly shunt dominated case, Reine's model appears applicable without any correction.

It is known that carrier density in accumulation layer increases by more than 4 orders of magnitude. Due to this, strong surface field exists which decreases the mobility value at the surface (compared to bulk) in addition to impurity scattering. To account for these effects, it was assumed that μ_{es} = 40.000 cm^2/Vs. The value has been taken from Refs. 2 and 5.

3.2. Effect of μ_{es} on responsivity

Figure 3(b) shows the plot of responsivity as a function of surface mobility μ_{es} for 2L, bulk (using full thickness t) and Reine's model. As expected, the responsivity of 2L model approaches to bulk model for μ_s approaching zero. However, there is difference of ~5% with Reine's model at μ_{es} = 10 cm^2/Vs and ~14% at $\mu_{es} = 10^4$ cm^2/Vs. The lower responsivity in Reine's model compared to bulk model stems from the fact that it uses the full thickness t whereas bulk model uses the corrected thickness, i.e., $t - t_s$ (or due to the $t_s/t << 1$ in Reine's case). It may be observed that this difference increases as μ_s increases beyond 10^4 cm^2/Vs. Hence it may be concluded that for μ_{es} nearing μ_b Reine' model may not be accurate enough.

3.3. Effect of S_r and α on responsivity

In the present model, as discussed earlier, device is split into bulk and surface regions. These are treated separately, e.g., photons that are absorbed in surface layer are assumed to have different mobility and lifetime values [Eq. (7)]. There will be redistribution of charge following absorption. Therefore, in practice, photo-generated holes will be repelled from +vely charged surface into bulk and thus reducing η_s. It is well know that the minority carrier lifetime in the surface region is a function of surface recombination velocity and thickness. Generally speaking, the quantum efficiency of the surface μ_s is much lower than that of the bulk μ_b. This individual magnitudes depend on the absorption coefficient and the thicknesses of the layers as follows

$$\eta_s = 1 - \exp(-\alpha t_s), \tag{36}$$

$$\eta_b = \exp(-\alpha t_s)\{1 - \exp[-\alpha(t - t_s)]\}. \tag{37}$$

The effective minority carrier lifetime τ_{eff} as a function of bulk lifetime τ_b and surface recombination velocity S_r (SRV), following Refs. 5 and 6 is given as

$$\frac{1}{\tau_{eff}} = \frac{1}{\tau_b} + \frac{S_r}{t}, \tag{38}$$

where S_r is a figure of merit for surface recombination. Hence, for real situations this lifetime should be used in the responsivity of surface layer. Furthermore, since the detector thickness is of the order of (or less) diffusion length, the carrier created in bulk can very well diffuse to the surface and recombine there. Hence, effective lifetime given in Eq. (38) should be used in bulk, surface or Reine's model for realistic situations which follows.

Using the realistic effective lifetime and quantum efficiencies given by Eqs. (36), (37), and (38) we next calculate the responsivities.

Figure 4 shows the plot of responsivity vs Q_{ss} for absorption coefficient of 500, 1000, 2000 cm^{-1} for fixed SRV of 1000 cm/s. The comparison of 2L and Reine's model is depicted. It may be seen 2L model predicts a higher responsivity than Reine's model particularly in the intermediate range of $1\times10^{10} < Q_{ss} < 1\times10^{12}$ cm^{-2}. Incidentally, this is the range obtained experimentally for various passivants such as anodic oxide, anodic floride, CdTe etc. used for PC n-HgCdTe detectors. It may be seen from this figure that for α of 2000 cm^{-1}, the maximum deviation between 2L and Reine's model is about 9% at the Q_{ss} of 1×10^{11} cm^{-2}. This deviation goes further up with the increase in α which will happen with the decrease in wavelength of radiation within the band of LWIR.

Figure 5 shows the plot of responsivity vs Q_{ss} for SRV of 100, 500, 1000 cm/s for fixed α of 1000 cm^{-1}. Again, the comparison of 2L and Reine's model is shown. Similar trends, as in Fig. 4 are obtained. It shows that effect of SRV and α on responsivity is similar. Furthermore, to give the idea that how much the shunt affects the bulk responsivity as a function of Q_{ss}, results of bulk model using full thickness t are also shown. It is clear from Figs. 3 and 4 that the inclusion of the shunt effect is important for $Q_{ss} < 5\times10^{11}$ cm^{-2}.

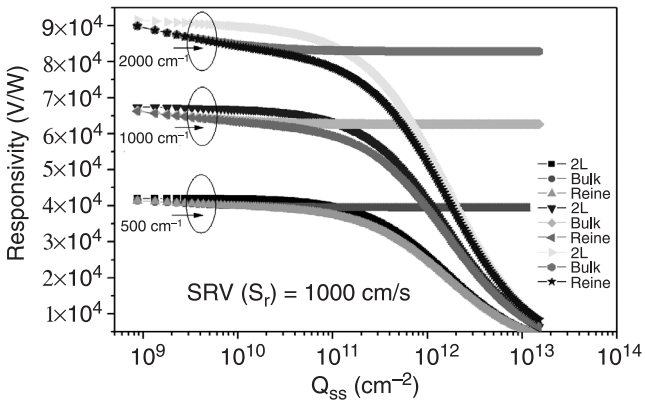

Fig. 4. The effect of absorption coefficient on responsivity for the fixed value of surface recombination velocity for 2L, bulk and Reine's model.

 © 2004 COSiW SEP, Warsaw

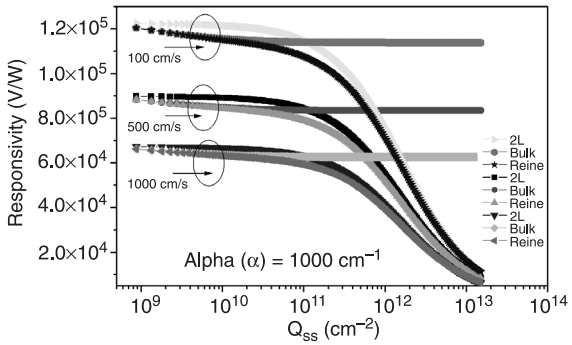

Fig. 5. The effect of surface recombination velocity on responsivity for the fixed value of absorption coefficient for 2L, bulk and Reine's model.

4. Conclusions

We have presented an improved two layer responsivity model for modelling the effect of shunt resistance in n-HgCdTe PC detectors. The model shows that for the values of Q_{ss} obtained experimentally in passivants used in these devices, the 2L model for realistic values predicts increased responsivity by 9% for Q_{ss} of 1×10^{11} cm^{-2} compared to Reine's model. A significant difference between the 2L model and Reine's model is seen for high α (i.e., low wavelength) whose surface effects become more dominant. This difference should be experimentally testable.

Acknowledgements

The authors are thankful to Director of SSPL for constant encouragement and permission to publish the paper.

References

1. R.M. Broudy and V.J. Mazurczyk, in *Semiconductors and Semimetals*, Vol. 18, pp. 157–99, edited by R.K. Willardson and A.C. Beer, Academic Press, New York, 1981.
2. M.B. Reine, K.R. Maschhoff, S.P. Tobin, P.W. Norton, J.A. Mroczkowski, and E.E. Kruger, *Semicond. Sci. Technol.* **8**, 788 (1993).
3. R. Pal, R.K. Bhan, K.C. Chhabra, and O.P. Agnihotri, *Semicond. Sci. Technol.* **11**, 231 (1996).
4. J.F. Silliquini, K.A. Fynn, B.D. Nener, L. Faraone, and R.A. Hartley, *Semicond. Sci. Technol.* **9**, 1515 (1994).
5. J.F. Silliquini and L. Faraone, *Semicond. Sci. Technol.* **12**, 1010 (1997).
6. R. Pal, B.L. Sharma, V. Gopal, V. Kumar, and O.P. Agnihotri, *IR Phys. and Technology* **40**, 101 (1999).
7. V. Dhar, R.K. Bhan, R. Ashokan, and V. Kumar, *Semicond. Sci. Technol.* **11**, 1302 (1996).
8. E.L. Dereniak and D.G. Crowe, *Optical Radiation Detectors*, John Wiley and Sons, New York, 1984, Ch. 4.
9. S.M. Sze, *Physics of Semiconductor Devices*, John Wiley and Sons, New York, Ch. 7, Sec. 7.2.1., 1981.

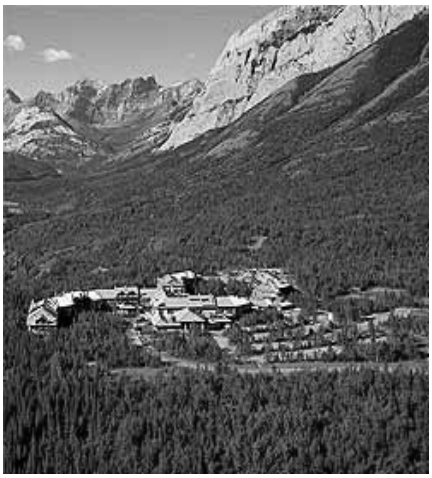

QWIP2004
International Workshop on Quantum Well Infrared Photodetectors

August 9–12, 2004
The Canadian Rockies
Delta Lodge at Kananaskis, Alberta

Chair: H.C.Liu
Co-chairs: S.D.Gunapala & H.Schneider

Advisory committee:
- Sumith Bandara – JPL USA
- Pallab Bhattacharya – U. Michigan USA
- Ph. Bois – Thales France
- Gail Brown – AFRL USA
- Anna Carbone – Polito Italy
- Dave Cardimona – AFRL USA
- E. Finkman – Technion Israel
- Bernhard Hirschauer – Acreo Sweden
- Vincent Larochelle – DRDC Canada
- Paul LeVan – AFRL USA
- Barbara McQuiston – QWIPTech USA
- Unil Perera – GSU USA
- Gabby Sarusi – Elop Israel
- Meimei Tidrow – BMDO USA
- Benny Toomarian – JPL USA

Workshop coordinator:
Tania Oogarah, Tel: 613 993–7116,
Fax: 613 990 0202,
E-mail: Tania.Oogarah@nrc.ca

Introduction:
This workshop is the third one of the series following QWIP2000 in Dana Point (USA) and QWIP2002 in Torino (Italy). QWIP is now a technology for infrared imaging, after rapid development in the past 15 years. It is also because of this rapid advance, some areas are not yet completely resolved and potentials are not fully exploited. The primary goal of this workshop is to gather all the experts in the QWIP R&D, government sponsors, industrial engineers, instrument technologists, end users, etc., and then discuss the current issues, formulate directions, and establish collaborations.

Scope:
- QWIP physics; for example, advanced or fully quantum mechanical QWIP model, realistic grating and optical coupler model, solutions to the slow response in low temperature and low background
- QWIP technology, for example, multicolor and multiband arrays
- QWIP applications, for example, military, medical/health, and commercial
- QWIP novel direction, for example, ultrahigh speed, two-photon response
- Related new approaches, for example quantum dots and other materials
- Related devices

Format:
The workshop is intended to provide a forum where ample time is allotted for presentation and discussion. The number of participants is limited to facilitate this goal. A good/basic prior knowledge of QWIP is assumed.

Tentative dates:
Abstract deadline: April 23, 2004
Notification of acceptance/rejection: May 14, 2004
Registration: June 23, 2004

 © 2004 COSiW SEP, Warsaw